

Quantum critical fluctuations generate intensely magnetic field–resilient superconductivity in UTe_2

Z. Wu,^{1†} T. I. Weinberger,^{1†} A. J. Hickey,¹ D. V. Chichinadze,²
D. Shaffer,³ A. Cabala,⁴ H. Chen,¹ M. Long,¹ T. J. Brumm,² W. Xie,⁵
Y. Lin,⁵, Y. Skourski,⁶ Z. Zengwei,⁵ D. E. Graf,² V. Sechovský,⁴
G. G. Lonzarich,¹ M. Vališka,⁴ F. M. Grosche,¹ A. G. Eaton^{1*}.

¹Cavendish Laboratory, University of Cambridge,
JJ Thomson Avenue, Cambridge, CB3 0HE, UK

²National High Magnetic Field Laboratory, Tallahassee, Florida 32310, USA

³Department of Physics, University of Wisconsin-Madison,
Madison, Wisconsin 53706, USA

⁴Charles University, Faculty of Mathematics and Physics, Department of
Condensed Matter Physics, Ke Karlovu 5, Prague 2, 121 16, Czech Republic

⁵Wuhan National High Magnetic Field Center, Wuhan 430074, China

⁶Hochfeld-Magnetlabor Dresden (HLD-EMFL),
Helmholtz-Zentrum Dresden-Rossendorf, Dresden, 01328, Germany

*Email: alex.eaton@phy.cam.ac.uk.

†These authors contributed equally to this work.

March 6, 2024

Quantum critical phase boundaries (QCPBs) – where a continuous phase transition occurs at zero temperature – have been found to nucleate novel electronic states in a number of strongly correlated materials.¹⁻³ Emergent electronic phases, such as unconventional superconductivity, frequently occur in close proximity to a QCPB.⁴⁻¹⁰ However, the antagonism between magnetic field and superconductivity generally suppresses such superconductive phases to modest magnetic field ranges, except in notable cases such as the high- T_c cuprates.^{10,11} Here we show that the heavy fermion Kondo-lattice system UTe_2 possesses a QCPB at remarkably high magnetic fields ~ 50 T, underpinning an extremely high field superconducting state that persists to fields > 70 T despite its relatively modest transition temperature of $T_c \approx 2$ K. Whereas previous studies¹²⁻¹⁹ found this superconducting state to exist exclusively inside a field-polarised paramagnetic host-phase accessed following a first-order metamagnetic transition, for magnetic field tilt angles in the rotation plane connecting the reciprocal (010) and (101) vectors, we find an extended region of this superconductivity outside the field-polarised state. In this special rotation plane we also observe a pronounced suppression of the metamagnetic transition towards zero temperature, revealing that the metamagnetic transition surface ends at a QCPB. The superconducting T_c exhibits a strong angular dependence and is enhanced close to the QCPB, where the onset of superconductivity is stretched over a surprisingly large magnetic field range reaching as low as 30 T. We model our data by a phenomenological Ginzburg-Landau theory, and show how an extended quantum critical line – rather than a more conventional QCPB at a singular point – anchors the remarkable high magnetic field phase landscape of UTe_2 .

Introduction

At absolute zero temperature, classical phases of matter are completely frozen in place. By contrast, in emergent electronic phases quantum zero-point motion allows for fluctuations to persist down to temperature $T = 0$ K. For sufficiently strong fluctuations a quantum phase transition may occur, typically from an ordered to a disordered state.¹⁻³ Depending on the dimensionality of the underlying phase space, such a transition may occur at a quantum critical point (QCP) or, in higher dimensions, across a continuous line or surface composed of QCPs.

Near a QCP, the enhancement of magnetic or density fluctuations can provide the pairing glue for unconventional superconducting phases to condense.⁴ For example, *d*-wave superconductivity is often found in proximity to antiferromagnetic (AFM) QCPs,^{10,11,20} whereas ferromagnetic (FM) QCPs can promote the formation of exotic *p*-wave superconductive phases.^{5,21,22} In a magnetic field the spin-degree of freedom of *p*-wave superconductors can yield complex multi-component superconducting phase diagrams.^{23,24} In some rare cases, such as the FM superconductor URhGe, the application of magnetic fields can even induce superconductivity close to a high magnetic field QCP.^{8,25,26}

The heavy fermion paramagnet UTe₂ crystallises in an orthorhombic body-centred lattice, with no evidence of long-range magnetic order above $T = 40$ mK (ref.²⁷). In zero applied magnetic field, $\mu_0 H$, a superconducting groundstate forms below a critical temperature $T_c = 2.1$ K (refs.^{12,28-30}). Despite the absence of FM order, this superconductive state exhibits multiple characteristics of odd-parity *p*-wave pairing^{12,28,31} analogous to its FM uranium-based cousins UGe₂, URhGe and UCoGe.^{5,21,22} The superconducting phase diagram of UTe₂ under applied magnetic field and pressure is astonishingly complex, with up to six distinct superconductive phases having been reported.^{12-14,32-34} The most remarkable of these phases is only found at extremely high magnetic field strengths, starting at $\mu_0 H \approx 40$ T and persisting to $\mu_0 H > 73$ T,

with a strong sensitivity to the orientation of magnetic field tilt angle.^{13,14,18,19}

This high- H superconductivity has been found to be entirely confined inside a field-polarised paramagnetic (PPM) host-phase, nestling against the PPM phase boundary within a narrow angular range for field tilted in the crystallographic $b - c$ plane.¹³⁻¹⁸ Recent measurements have also confirmed its existence for a magnetic field component tilted away from the $b - c$ plane towards the a -axis¹⁹ – but again, this exotic high- H superconductivity was exclusively found inside the PPM state. The metamagnetic transition into the PPM state has been found to be strongly first-order at low temperatures for the orientations measured so far.

Here, we probe the high- H phase diagram of UTe_2 with contacted and contactless electrical conductivity measurements on a new generation of pristine quality samples.^{30,35-37} We find an extended range of the high- H superconductive state in the multi-dimensional $H_{a,b,c}$ phase space, where H_i denotes the magnetic field oriented parallel to the crystallographic i direction. Strikingly, for rotations in the $b-abc-ac$ plane (explicitly defined as tilting the magnetic field to point along each of the reciprocal (010), (111) and (101) vectors) we uncover an extended range of superconductivity at $\mu_0 H \approx 40$ T that extends below the PPM. Non-Ohmic current-voltage characteristics identifying the onset region of SC3 extend as low as $\mu_0 H = 30$ T. This angular range at which the onset is pushed to minimal field coincides with the orientation at which we observe the first-order metamagnetic (MM) transition to the PPM being suppressed towards zero temperature, producing a MM quantum critical end point. In combination, our high- H measurements (i) identify a quantum critical boundary (the QCPB) to the surface of first-order metamagnetic transitions in \vec{H} -space at the remarkably high magnetic field scale of ~ 50 T, (ii) anchor the field-resilient superconductivity in UTe_2 close to this boundary, and (iii) reveal that in a narrow field range close to the QCPB the onset of field-resilient superconductivity can reach to fields that lie far below the MM transition field.

Results

Figure 1 summarises our high- H measurements of the superconducting phase landscape of UTe_2 . We label the superconducting groundstate accessed at $\mu_0 H = 0$ T as SC1 (in blue), while the pink region identifies a distinct superconducting state³⁸ attained for $\mu_0 H_b \lesssim 35$ T (SC2) that shares some region of coexistence with SC1.³⁹ The focus of the present study is the purple SC3 phase, which spans an extended region in the $H_{a,b,c}$ phase space both inside the PPM state (coloured orange) and below it.

The phase landscape of Fig. 1 is constructed in part from the data in Figure 2. Up to the maximum applied field of the magnet system utilised for this suite of measurements, of 41.5 T, for incremental magnetic field tilt angles rotating from b towards ca at $T = 0.4$ K we suddenly access the SC3 state at $\theta_{b-ac} = 17.5^\circ$. In Fig. 2b we define the purple SC3 region by the observation of zero resistivity ρ (in the low current limit). Interestingly, we observe a broadening of the onset of the SC3 phase for successively higher rotation angles θ_{b-ac} , identified as the turning over of $\rho(H)$ from a positive to a negative gradient. This onset extends down to a minimum magnetic field of ≈ 30 T at $\theta_{b-ac} \approx 34^\circ$, before progressing back up to higher fields for further inclination in the $b - ac$ plane. This wide magnetic field domain of negatively sloped magnetoresistance exhibits a highly non-linear relationship between excitation current and probed voltage (Fig. 2e,f), indicating the likely presence of exotic vortex dynamics. We therefore identify a broad range of the UTe_2 high field phase diagram, in this special rotation plane, to be occupied by the onset of the SC3 phase.

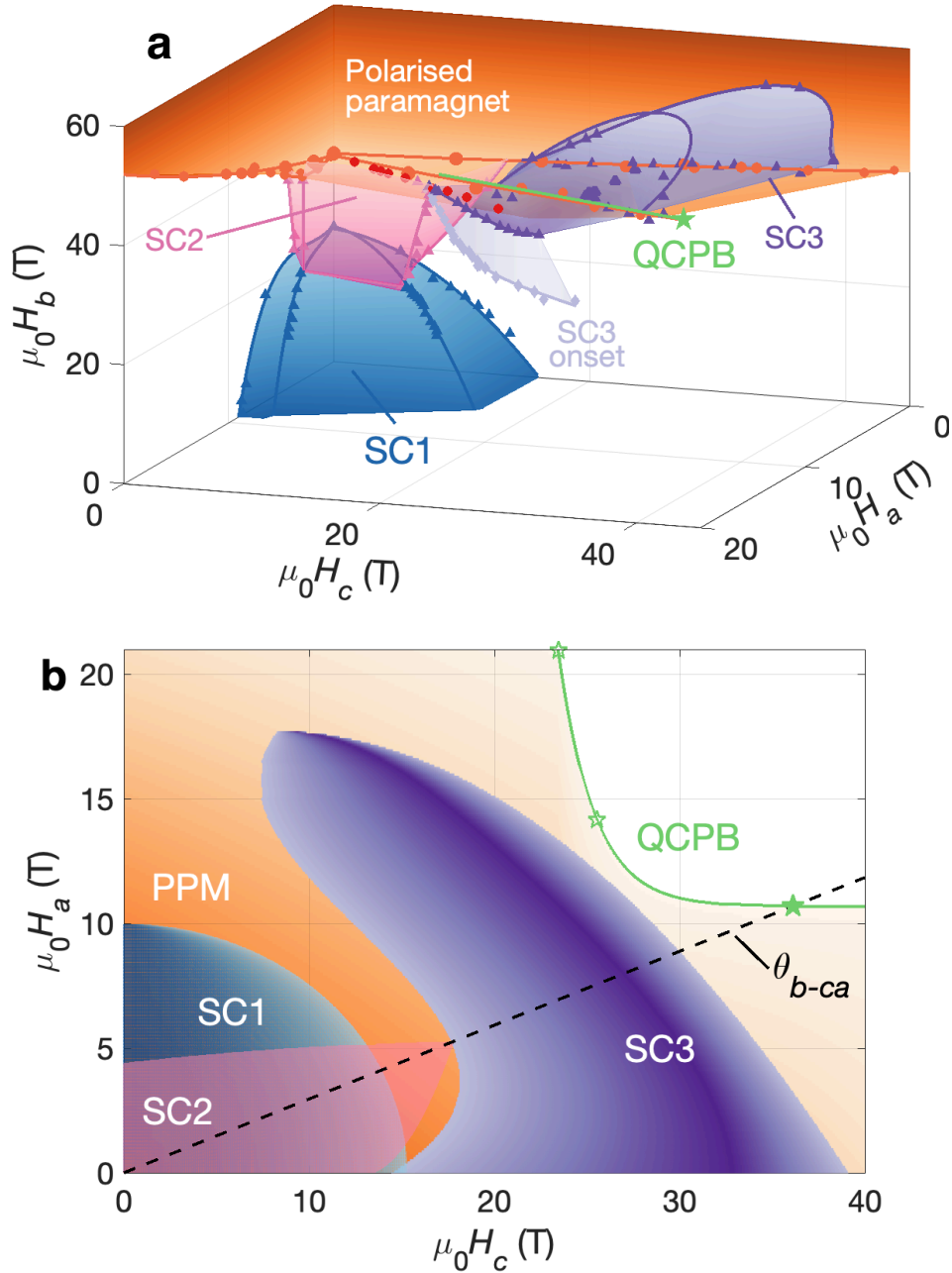


Fig. 1. The high magnetic field phase landscape of UTe_2 . **a**, Three superconducting phases are identified, labelled SC1 (blue), SC2 (pink) and SC3 (purple). Orange and red points demarcate a metamagnetic transition to the field-polarised paramagnetic state only accessible in high magnetic field strengths of $\mu_0 H_b > 34$ T. Data points identifying superconducting phase boundaries are from measurements at $T = 0.3\text{-}0.7$ K while those for the polarised paramagnet (PPM) are taken at $T = 4\text{-}6$ K. Each data point corresponds either to a magnetic field sweep of a dc magnet, or to a pulsed field measurement. Lines and surfaces are guides to the eye. The quantum critical phase boundary (QCPB) stems from where the first-order transition to the PPM is suppressed to 0 K, identified by the green star and marked by the green line that bends upwards out of the plane of the page.

Fig. 1. (cont.) **b**, Bird's-eye view of the phase diagram down along the $H||b$ direction, illustrating the extent of the superconducting phases and the location of the critical boundary to the metamagnetic transition surface. The approximate location of the critical boundary has been inferred from our high-field measurements along the rotation trajectory, and is indicated by the green line (and solid star) and from high field transport data in ref. ¹⁹ (open stars).

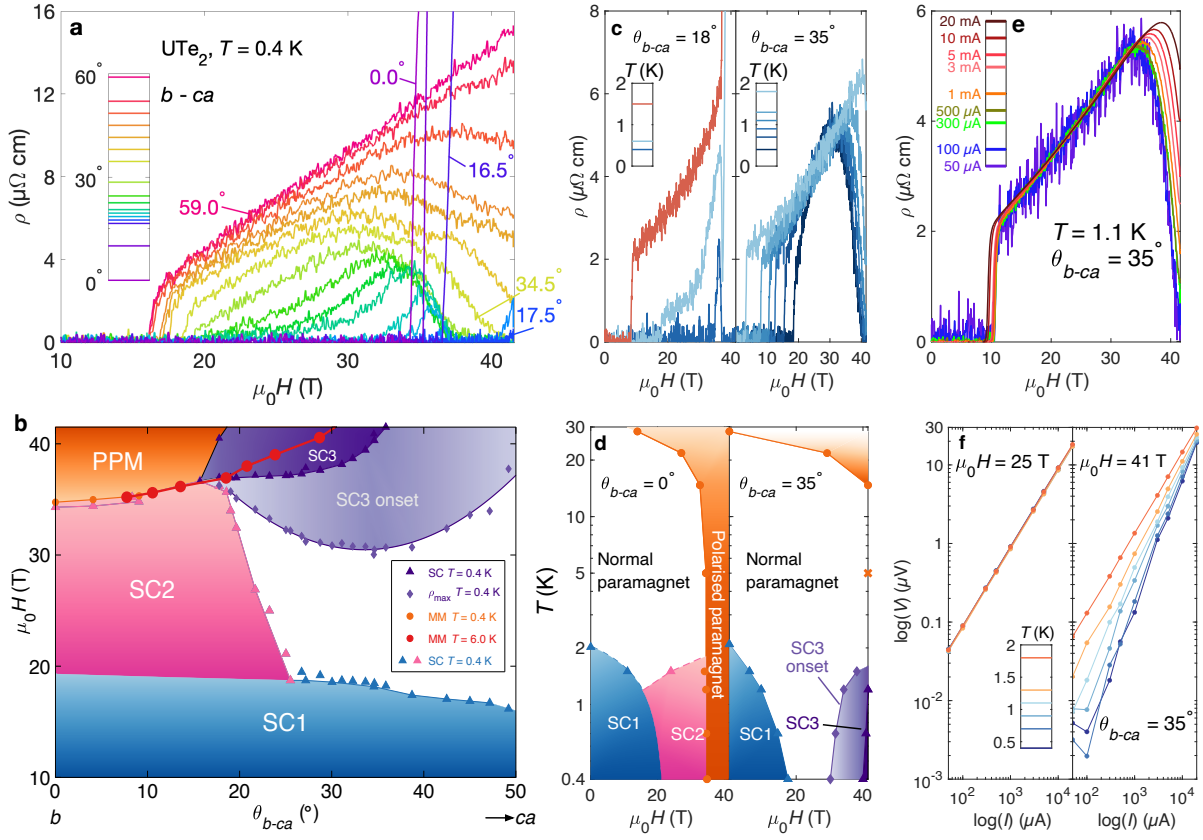


Fig. 2. Spillover of SC3 outside the polarised paramagnetic phase. **a**, Electrical resistivity ρ versus $\mu_0 H$ at successive magnetic field tilt angles in the $b-abc-ca$ rotation plane at $T = 0.4$ K. At $\theta_{b-ca} = 17.5^\circ$ zero resistance is observed over the field interval of $0 \text{ T} \leq \mu_0 H \leq 41 \text{ T}$ as each of SC1, SC2 and SC3 are successively accessed. **b**, The phase landscape of UTe_2 plotted radially in θ_{b-ca} . An extended region of the onset of SC3 is observed outside the PPM state, identified by the turning over from positively to negatively sloped $\rho(H)$ in panel (a). The red circles defining the PPM boundary were measured above T_c^{SC3} . **c**, A comparison of the temperature sensitivity of SC3 at $\theta_{b-ca} = 18^\circ$ (left) and $\theta_{b-ca} = 35^\circ$ (right). On the edge of the SC3 dome at $\theta_{b-ca} = 18^\circ$ the T_c is only ≈ 0.6 K, whereas at $\theta_{b-ca} = 35^\circ$ SC3 is much more robust to elevated temperatures. **d**, The evolution of the SC1, SC2, SC3 and PPM phases for $\theta_{b-ca} = 0^\circ$ (left) and $\theta_{b-ca} = 35^\circ$ (right). At $\theta_{b-ca} = 35^\circ$ the melting of PPM is not observed at 5 K (marked by a cross – see Supplementary Information for a detailed discussion of the raw data that construct this panel). This shows that SC3 extends outside the PPM state in this special rotational plane. **e**, Effective resistivity at $\theta_{b-ca} = 35^\circ$ for different excitation currents as indicated. **f**, Log-log plot of voltage V versus current I from 0.4-1.8 K at $\theta_{b-ca} = 35^\circ$. Ohmic $I - V$ characteristics are observed in the normal paramagnetic state at $\mu_0 H = 25 \text{ T}$, whereas at $\mu_0 H = 41 \text{ T}$ the $I - V$ behaviour is highly non-Ohmic. We therefore identify the turning over of the $\rho(H)$ traces in (a) as marking the onset of SC3, characterised by this markedly non-linear relationship between I and V .

For $H \parallel b$, the first-order MM transition to the PPM is observed at $\mu_0 H_m \approx 34.5$ T in the zero temperature limit.^{16,36,40,41} On warming, this transition passes a critical end point at ≈ 10 K and evolves into a broad crossover, characterised by e.g. a maximum in $\rho(H)$ (refs.^{12,13,16,40,42}). The transition gradually melts, moving down to lower values of H_m with increasing temperature up to ≈ 30 K whereat it is suppressed to 0 T. We plot this schematically in Fig. 2d for $H \parallel b$ (i.e. $\theta_{b-ca} = 0^\circ$), along with the corresponding phase landscape for $\theta_{b-ca} = 35^\circ$. Strikingly, upon warming above T_c^{SC3} at this angle, we do not observe a signature of the PPM state in our accessible field range of $\mu_0 H \leq 41.5$ T until $T > 10$ K (see Supplementary Information for raw data and extended discussion). Furthermore, we performed a series of rotations in the $b - ca$ plane at 6 K – to suppress all superconducting states and therefore solely probe the PPM phase – to map out the boundary of the MM transition in this plane, which we plot as red circles in Fig. 2b (see Supplementary Information). The MM transition clearly bisects a substantive region of SC3. Therefore, our measurements have uncovered that an extended range of SC3 – and its broad onset region – extends considerably outside the PPM state in the $b - ca$ plane. This is in stark contrast to prior measurements of SC3 in the $b - c$ plane that observed SC3 exclusively within the PPM host-state.^{13–18}

This motivates a closer examination of the nature of the field-induced MM phase transition in UTe_2 , to which we now turn. In the FM superconductor URhGe, magnetic field-induced superconductivity is found at a QCPB characterised by the suppression of a first-order MM transition to zero temperature.⁸ In Figure 3 we map the evolution of the UTe_2 MM transition through contactless resistivity measurements by the PDO technique (see Methods) in pulsed magnetic fields. All data are at $T = 4.2$ K, with three sequences of rotations performed tilting H away from b towards each of a , c , and ac . We performed these measurements on the same sample, to minimise any variations in sample properties.

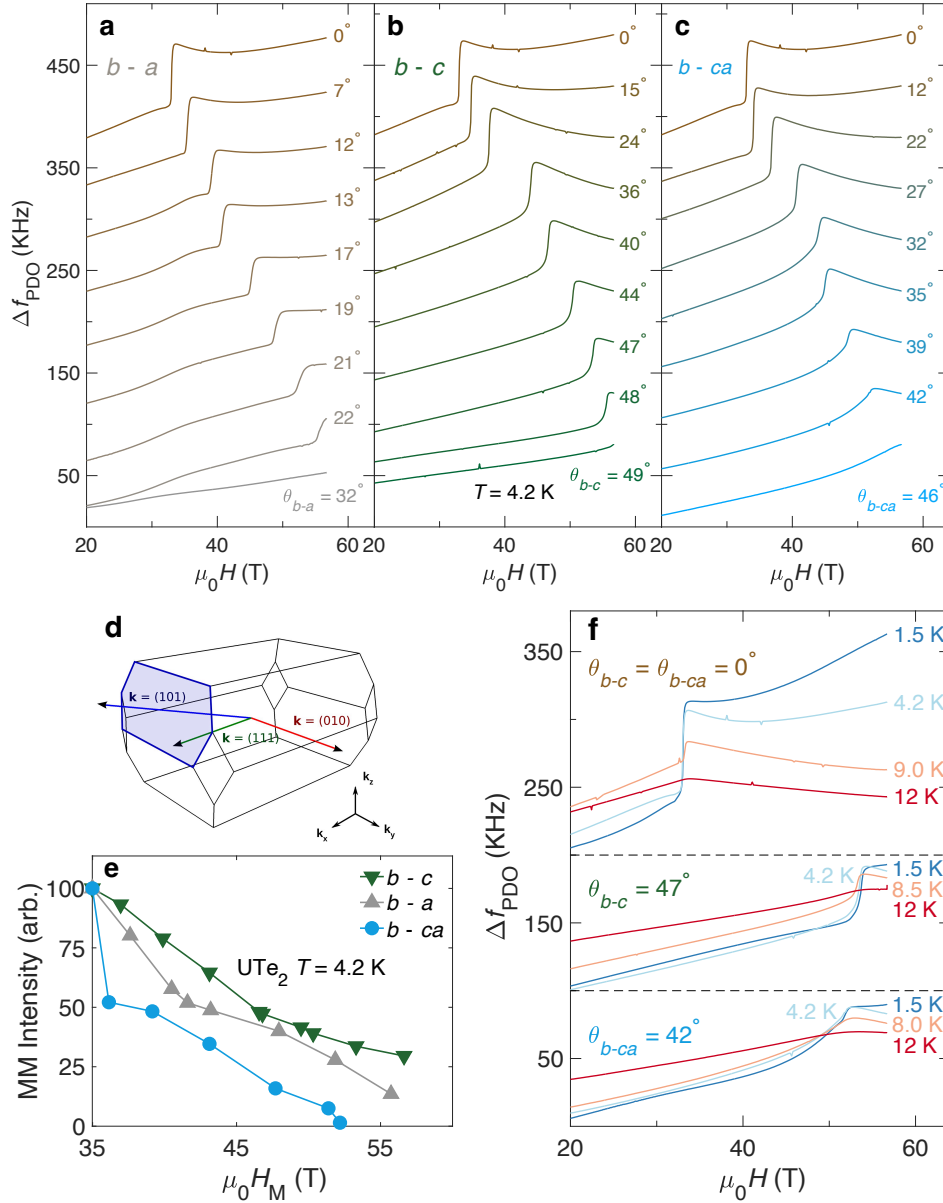


Fig. 3. Suppression of the first order metamagnetic phase transition towards zero temperature. Contactless conductivity measurements measured in pulsed magnetic fields by the PDO technique, rotating from $H \parallel b$ towards **a**, $H \parallel a$, **b**, $H \parallel c$ and **c**, $H \parallel ca$. All data were collected on the same sample at $T = 4.2$ K. When the MM transition field $\mu_0 H_m \approx 50$ T, in the $b - a$ and $b - c$ planes the transition is still relatively sharp and first order-like. By contrast, in the $b - ca$ plane it has softened markedly and looks considerably more second order-like at $\theta_{b-ca} = 42^\circ$. **d**, Schematic defining the $b - abc - ca$ rotation plane as the arc traced by rotating through the (010), (111) and (101) reciprocal-space vectors. **e**, Intensity of the MM transition for the three rotation planes in (a-c) (see Supplementary Information). **f**, Temperature evolution for H oriented $\parallel b$ and at $\theta_{b-c} = 47^\circ$ and $\theta_{b-ca} = 42^\circ$. The 1.5 K curve at $\theta_{b-ca} = 42^\circ$ looks similar in profile to the 12 K trace at $\theta_{b-ca} = 0^\circ$; furthermore, while $\theta_{b-ca} = 42^\circ$ and $\theta_{b-c} = 47^\circ$ have very similar values of H_m , it is clear that $\theta_{b-ca} = 42^\circ$ is softer and thus lies closer to the QCPB.

At $\theta_{b-a} = \theta_{b-c} = \theta_{b-ca} = 0^\circ$ (i.e. $H \parallel b$) the MM transition in the contactless resistivity is sharp and first order-like in character, consistent with prior studies.^{14,36,43,44} Tilting the magnetic field in the $b - a$ and $b - c$ planes, the magnitude of the jump in the PDO frequency shift Δf_{PDO} decreases at higher rotation angles. However, it is still identified as a sharp jump even at $\mu_0 H_m \approx 50$ T in both of these planes. In marked contrast, in the $b - ca$ plane the MM transition undergoes a pronounced softening at inclination angles of $\theta_{b-ca} \approx 40^\circ$, with the jump being strongly suppressed and becoming much more second order-like (Fig. 3c). We plot the temperature variation of three H -orientations in Fig. 3f. It is clear that in the $b - ca$ rotation plane the first-order MM transition is suppressed towards zero temperature much more rapidly than in either the $b - a$ or $b - c$ planes. Similar to the case of URhGe, this is characteristic of crossing a QCPB.⁸ We note that recent high- H measurements of UTe₂ reported in ref.¹⁹ are consistent with our finding, and indeed provide corroborating evidence for the existence of an extended quantum critical line in the multidimensional phase landscape. This is seen by the suppression of the MM transition upon rotating towards a at fixed $\theta_{b-c} = 23^\circ$ and $\theta_{b-c} = 30^\circ$ (see Supplementary Information for a detailed comparison of our measurements with those of ref.¹⁹).

Strikingly, this angular range over which the MM transition is markedly suppressed coincides with the magnetic field orientation over which the SC3 onset occurs at minimal H (Fig. 2a,b). Therefore, our measurements provide strong evidence for the presence of an extended range of quantum critical fluctuations, at the remarkably high magnetic field scale of ~ 50 T, underpinning the formation of the exotic SC3 superconductive state of UTe₂.

Discussion

As prior high- H measurements of UTe₂ in the $b - c$ plane only observed SC3 inside the PPM, the field-induced compensation of magnetic exchange was proposed as a possible microscopic

origin.¹⁸ However, our finding of the zero resistance SC3 state extending outside the PPM – accompanied by an extended field region of the onset of SC3 even further away from the MM phase transition line – argues strongly against this scenario being the sole mechanism. The extremely high- H scale of SC3 led to another interesting theoretical proposal based on Hofstadter physics – similar to prior considerations of Landau quantization driving H -reentrant superconductivity⁴⁵ – but the recent observation of SC3 surviving in exceptionally disordered crystals⁴⁶ argues strongly against coherent Landau quantization.

To identify the likely source of the magnetic fluctuations driving the formation of SC3, we model the MM phase transition to the PPM state using a Ginzburg-Landau theory:

$$\mathcal{F}[\mathbf{M}](\mathbf{H}) = \frac{1}{2}\chi_i^{-1}M_i^2 + \frac{1}{4}\beta_{ij}M_i^2M_j^2 + \frac{1}{6}\gamma M_y^6 - \mathbf{M} \cdot \mathbf{H} \quad (1)$$

where $i, j = x, y, z$, \mathbf{M} is the magnetic order parameter (magnetization), and χ_i^{-1} , β_{ij} , and γ are Ginzburg-Landau parameters^{43,47,48}. The parameters are chosen such that at zero applied field the free energy has two minima: a global paramagnetic minimum at $|\mathbf{M}| = 0$, and a minimum with higher energy at $\mathbf{M} = \mathbf{M}_*$ pointing along the b direction, corresponding to the PPM phase. Applying an external magnetic field lowers the minimum at \mathbf{M}_* until it becomes the new global minimum at the MM phase transition field H_m . The condition for the local minimum to exist is $\beta_{yy} < 0$; a critical end point (CEP) thus arises when β_{yy} changes sign at some temperature T_0 . The CEP generally appears at $T_{CEP} \lesssim T_0$, and in UTe₂ is located at ≈ 10 K for $H \parallel b$ (refs.^{40,42}).

To leading order close to T_0 the temperature dependence of the GL coefficients can be modeled phenomenologically as⁴⁷

$$\begin{aligned} \chi_i^{-1}(T) &\propto 1 + bT^2 - bcT^4 \\ \beta_{ij}(T) &\propto 1 - cT^2 \end{aligned} \quad (2)$$

In principle, the b and c coefficients carry i, j indices, but the only ones relevant for T_{CEP} are $i = j = y$. Generally, b and c are also functions of the direction of the applied magnetic field,

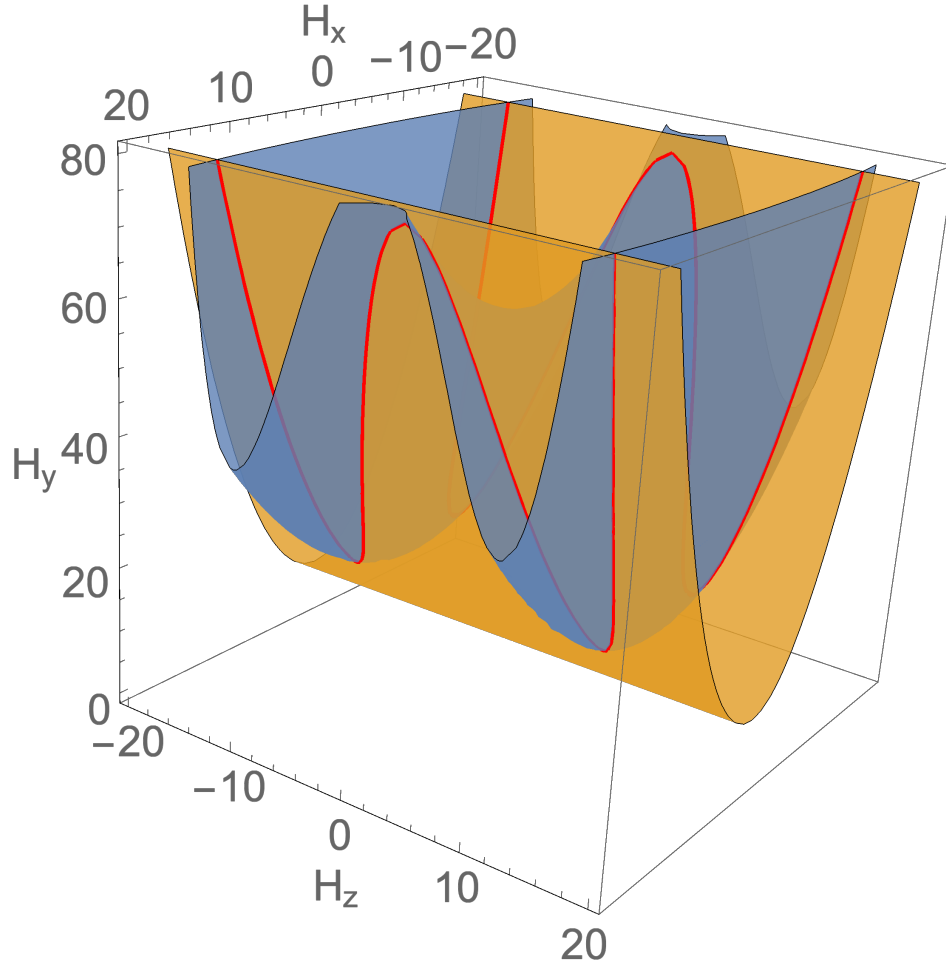


Fig. 4. QCPB phenomenological theory. Cartoon sketch of the QCPB line (red) in the space of magnetic field components H_j in arbitrary units, determined by the intersection of the MM phase transition boundary (orange) and the locus of points at which $T_0 = 0$ (blue).

such that $T_0(\mathbf{H}) = 1/\sqrt{c(\mathbf{H})} = 0$ at some \mathbf{H}_{QCP} (at which c diverges), leading to a QCPB with $T_{CEP} \propto T_0 \rightarrow 0$ K. Importantly, following this treatment we expect a line of critical points since $c^{-1}(\mathbf{H}_*) = 0$ defines a 2D surface that intersects the MM transition surface along an extended quantum critical line. Thereby, this model accurately captures the geometrical qualities of the high- H quantum critical landscape of UTe_2 probed by our experiments. Furthermore, as for the case of FM uranium-based superconductors such as URhGe, high-field re-entrant superconduc-

tivity in such a setting is expected to occur on both sides of the QCPB.^{8,26,48} Our observation of SC3 on both sides of the MM transition of UTe₂ therefore provides strong evidence, in addition to the pronounced suppression of the MM transition towards zero temperature, in favour of a quantum critical origin for SC3.

Our study of the high- H phase space of UTe₂ at ambient pressure poses the natural corollary of: how does this quantum critical phase landscape evolve under pressure? The pressure dependences of the specific heat and electrical resistivity of UTe₂ have led to the proposal that an AFM QCP is located at a critical pressure of $p_c \approx 1.45$ GPa, beyond which the superconducting groundstate(s) are abruptly truncated^{12,32,49} and incommensurate AFM order is stabilised.⁵⁰ $\mu_0 H_m$ decreases under pressure, and an intriguing H -induced superconducting state – which appears to bear numerous similarities with the ambient pressure SC3 state and persists to high fields – has been observed at pressures above p_c for $H \parallel c$.³³ Given the remarkable complexity of the ambient pressure phase landscape uncovered by our measurements, a promising new route to understanding the multitude of distinct superconducting states^{31–33} in UTe₂ lies in tracking the evolution of the QCPB we report here, and its associated Widom lines, in relation to the numerous superconducting phase boundaries spanning the multidimensional pressure–temperature– $H_{a,b,c}$ phase landscape.

References

- [1] Sachdev, S. Quantum phase transitions. *Phys. World* **12**, 33 (1999).
- [2] Coleman, P. & Schofield, A. J. Quantum criticality. *Nature* **433**, 226–229 (2005).
- [3] Gegenwart, P., Si, Q. & Steglich, F. Quantum criticality in heavy-fermion metals. *Nat. Phys.* **4**, 186–197 (2008).
- [4] Monthoux, P., Pines, D. & Lonzarich, G. G. Superconductivity without phonons. *Nature* **450**, 1177–1183 (2007).
- [5] Saxena, S. S. *et al.* Superconductivity on the border of itinerant-electron ferromagnetism in UGe₂. *Nature* **406**, 587–592 (2000).
- [6] Schröder, A. *et al.* Onset of antiferromagnetism in heavy-fermion metals. *Nature* **407**, 351–355 (2000).
- [7] Custers, J. *et al.* The break-up of heavy electrons at a quantum critical point. *Nature* **424**, 524–527 (2003).
- [8] Lévy, F., Sheikin, I. & Huxley, A. Acute enhancement of the upper critical field for superconductivity approaching a quantum critical point in URhGe. *Nat. Phys.* **3**, 460–463 (2007).
- [9] Dai, J., Si, Q., Zhu, J.-X. & Abrahams, E. Iron pnictides as a new setting for quantum criticality. *Proc. Natl. Acad. Sci. USA* **106**, 4118–4121 (2009).
- [10] Michon, B. *et al.* Thermodynamic signatures of quantum criticality in cuprate superconductors. *Nature* **567**, 218–222 (2019).
- [11] Keimer, B., Kivelson, S. A., Norman, M. R., Uchida, S. & Zaanen, J. From quantum matter to high-temperature superconductivity in copper oxides. *Nature* **518**, 179–186 (2015).
- [12] Aoki, D. *et al.* Unconventional superconductivity in UTe₂. *J. Phys. Condens. Matter* **34**, 243002 (2022).
- [13] Lewin, S. K., Frank, C. E., Ran, S., Paglione, J. & Butch, N. P. A Review of UTe₂ at High Magnetic Fields. *Rep. Prog. Phys.* (2023).
- [14] Ran, S. *et al.* Extreme magnetic field-boosted superconductivity. *Nat. Phys.* **15**, 1250–1254 (2019).
- [15] Knafo, W. *et al.* Comparison of two superconducting phases induced by a magnetic field in UTe₂. *Commun. Phys.* **4**, 40 (2021).

- [16] Miyake, A. *et al.* Enhancement and Discontinuity of Effective Mass through the First-Order Metamagnetic Transition in UTe_2 . *J. Phys. Soc. Jpn.* **90**, 103702 (2021).
- [17] Schönemann, R. *et al.* Sudden adiabaticity signals reentrant bulk superconductivity in UTe_2 . *PNAS Nexus* **3**, pgad428 (2024).
- [18] Helm, T. *et al.* Field-induced compensation of magnetic exchange as the possible origin of reentrant superconductivity in UTe_2 . *Nat. Commun.* **15**, 37 (2024).
- [19] Lewin, S. K. *et al.* High-Field Superconducting Halo in UTe_2 (2024). [arXiv:2402.18564](https://arxiv.org/abs/2402.18564).
- [20] Mathur, N. *et al.* Magnetically mediated superconductivity in heavy fermion compounds. *Nature* **394**, 39–43 (1998).
- [21] Aoki, D. *et al.* Coexistence of superconductivity and ferromagnetism in URhGe. *Nature* **413**, 613–616 (2001).
- [22] Slooten, E., Naka, T., Gasparini, A., Huang, Y. K. & de Visser, A. Enhancement of Superconductivity near the Ferromagnetic Quantum Critical Point in UCoGe. *Phys. Rev. Lett.* **103**, 097003 (2009).
- [23] Joynt, R. & Taillefer, L. The superconducting phases of UPt_3 . *Rev. Mod. Phys.* **74**, 235–294 (2002).
- [24] Leggett, A. J. A theoretical description of the new phases of liquid ^3He . *Rev. Mod. Phys.* **47**, 331–414 (1975).
- [25] Lévy, F., Sheikin, I., Grenier, B. & Huxley, A. D. Magnetic field-induced superconductivity in the ferromagnet URhGe. *Science* **309**, 1343–1346 (2005).
- [26] Yelland, E., Barraclough, J., Wang, W., Kamenev, K. & Huxley, A. High-field superconductivity at an electronic topological transition in URhGe. *Nat. Phys.* **7**, 890–894 (2011).
- [27] Azari, N. *et al.* Absence of Spontaneous Magnetic Fields due to Time-Reversal Symmetry Breaking in Bulk Superconducting UTe_2 . *Phys. Rev. Lett.* **131**, 226504 (2023).
- [28] Ran, S. *et al.* Nearly ferromagnetic spin-triplet superconductivity. *Science* **365**, 684–687 (2019).
- [29] Aoki, D. *et al.* Unconventional Superconductivity in Heavy Fermion UTe_2 . *J. Phys. Soc. Jpn.* **88**, 43702 (2019).
- [30] Sakai, H. *et al.* Single crystal growth of superconducting UTe_2 by molten salt flux method. *Phys. Rev. Mater.* **6**, 073401 (2022).

- [31] Kinjo, K. *et al.* Superconducting spin reorientation in spin-triplet multiple superconducting phases of UTe_2 . *Sci. Adv.* **9**, eadg2736 (2023).
- [32] Braithwaite, D. *et al.* Multiple superconducting phases in a nearly ferromagnetic system. *Communications Physics* 2019 2:1 **2**, 1–6 (2019).
- [33] Aoki, D. *et al.* Multiple superconducting phases and unusual enhancement of the upper critical field in UTe_2 . *J. Phys. Soc. Jpn.* **89**, 053705 (2020).
- [34] Honda, F. *et al.* Pressure-induced Structural Phase Transition and New Superconducting Phase in UTe_2 . *J. Phys. Soc. Jpn.* **92**, 044702 (2023).
- [35] Eaton, A. G. *et al.* Quasi-2D Fermi surface in the anomalous superconductor UTe_2 . *Nat. Commun.* **15**, 223 (2024).
- [36] Wu, Z. *et al.* Enhanced triplet superconductivity in next generation ultraclean UTe_2 (2023). arXiv:2305.19033.
- [37] Aoki, D. Molten Salt Flux Liquid Transport Method for Ultra Clean Single Crystals UTe_2 (2024). arXiv:2402.12740.
- [38] Rosuel, A. *et al.* Field-Induced Tuning of the Pairing State in a Superconductor. *Phys. Rev. X* **13**, 011022 (2023).
- [39] Sakai, H. *et al.* Field Induced Multiple Superconducting Phases in UTe_2 along Hard Magnetic Axis. *Phys. Rev. Lett.* **130**, 196002 (2023).
- [40] Miyake, A. *et al.* Metamagnetic Transition in Heavy Fermion Superconductor UTe_2 . *J. Phys. Soc. Jpn.* **88** (2019).
- [41] Aoki, D. *et al.* Field-Induced Superconductivity near the Superconducting Critical Pressure in UTe_2 . *J. Phys. Soc. Jpn.* **90**, 074705 (2021).
- [42] Vališka, M. *et al.* Dramatic elastic response near the critical end point of the itinerant metamagnets (2023). arXiv:2307.01884.
- [43] Lin, W.-C. *et al.* Tuning magnetic confinement of spin-triplet superconductivity. *npj Quantum Mater.* **5**, 68 (2020).
- [44] Ran, S. *et al.* Expansion of the high field-boosted superconductivity in UTe_2 under pressure. *npj Quantum Mater.* **6**, 75 (2021).
- [45] Rasolt, M. and Tessanovic, Z. Theoretical aspects of superconductivity in very high magnetic fields. *Rev. Mod. Phys.* **64**, 709–754 (1992).

- [46] Frank, C. E. *et al.* Orphan High Field Superconductivity in Non-Superconducting Uranium Ditelluride (2023). arXiv:[2304.12392](https://arxiv.org/abs/2304.12392).
- [47] Yamada, H. Metamagnetic transition and susceptibility maximum in an itinerant-electron system. *Phys. Rev. B* **47**, 11211–11219 (1993).
- [48] Mineev, V. P. Reentrant superconductivity in URhGe. *Phys. Rev. B* **91**, 014506 (2015).
- [49] Thomas, S. M. *et al.* Evidence for a pressure-induced antiferromagnetic quantum critical point in intermediate-valence UTe₂. *Sci. Adv.* **6**, 8709–8723 (2020).
- [50] Knafo, W. *et al.* Incommensurate antiferromagnetism in UTe₂ under pressure (2023). arXiv:[2311.05455](https://arxiv.org/abs/2311.05455).